1	Focusing and non-focusing modulation strategies for the improvement
2	of on-line two-dimensional hydrophilic interaction chromatography $ imes$
3	reversed phase profiling of complex food samples.
4	Lidia Montero <sup>a</sup> , Elena Ibáñez <sup>a</sup> , Mariateresa Russo <sup>b</sup> , Luca Rastrelli <sup>c</sup> , Alejandro
5	Cifuentes <sup>a</sup> , Miguel Herrero <sup>a*</sup>
6	<sup>a</sup> Laboratory of Foodomics, Institute of Food Science Research (CIAL-CSIC), Nicolás
7	Cabrera 9, 28049 - Madrid, Spain
8	<sup>b</sup> Laboratory of Food Chemistry, Dipartimento di Agraria (QuaSic.A.Tec.), Università
9	Mediterranea di Reggio Calabria, Reggio Calabria, loc. Feo di Vito, 89122 -
10	Reggio Calabria, Italy
11	<sup>c</sup> Dipartimento di Farmacia, Università di Salerno, Via Giovanni Paolo II 132, 84084 -
12	Fisciano, Italy
13	
14	
15	
16	
17	
18 19 20	Corresponding author: m.herrero@csic.es (M. Herrero) TEL: +34 910 017 946 FAX: +34 910 017 905

# 21 ABSTRACT.

22 Comprehensive two-dimensional liquid chromatography (LC  $\times$  LC) is ever gaining 23 interest in food analysis, as often, food-related samples are too complex to be analyzed 24 through one-dimensional approaches. The use of hydrophilic interaction chromatography 25 (HILIC) combined with reversed phase (RP) separations has already been demonstrated 26 as a very orthogonal combination, which allows attaining increased resolving power. 27 However, this coupling encompasses different analytical challenges, mainly related to the 28 important solvent strength mismatch between the two dimensions, besides those common 29 to every  $LC \times LC$  method. In the present contribution, different strategies are proposed 30 and compared to further increase HILIC  $\times$  RP method performance for the analysis of 31 complex food samples, using licorice as a model sample. The influence of different 32 parameters in non-focusing modulation methods based on sampling loops, as well as 33 under focusing modulation, through the use of trapping columns in the interface and 34 through active modulation procedures are studied in order to produce resolving power 35 and sensitivity gains. Although the use of a dilution strategy using sampling loops as well 36 as the highest possible first dimension sampling rate allowed significant improvements 37 on resolution, focusing modulation produced significant gains also in peak capacity and 38 sensitivity. Overall, the obtained results demonstrate the great applicability and potential 39 that active modulation may have for the analysis of complex food samples, such as 40 licorice, by HILIC  $\times$  RP.

41

42 Keywords: Metabolite profiling, two-dimensional LC, licorice, active modulation,
 43 trapping columns, resolution.

## 45 **1. INTRODUCTION**

46 The use of multidimensional liquid chromatography (MDLC) within the food analysis 47 field is gaining interest, as foods and food-related products are normally considered as 48 very complex matrices [1]. Indeed, it is frequent to find food samples that are simply too 49 complex to be analyzed by conventional one-dimensional chromatography. In other 50 cases, food-related samples may not be so complex in terms of number of compounds 51 present, but these could be composed by mixtures of closely related components that are 52 also difficult to be resolved. Although there are several approaches to MDLC of food, the 53 use of comprehensive two-dimensional liquid chromatography (LC  $\times$  LC) coupled on-54 line, presents different advantages over off-line modes as well as over other couplings, 55 such as heart-cutting two-dimensional LC. Most-notably, faster separations may be 56 obtained with high resolving power in a fully-automated way, thus, increasing robustness 57 and reproducibility [2,3]. However, the optimization of a LC  $\times$  LC method is far from 58 being easy, as there are different inter-related parameters which modification may directly 59 influence others [4]. These optimization challenges are even more pronounced when 60 orthogonal separation mechanisms are coupled, which in practice, is the most-interesting 61 approach. By selecting two independent non-correlated separation modes in both 62 dimensions, significant gains on resolving power and peak capacity are potentially attainable. However, using two very different separation mechanisms in both dimensions 63 64 means that important solvent incompatibility and/or immiscibility problems may be 65 found. The combination between hydrophilic interaction chromatography (HILIC) in the first dimension (<sup>1</sup>D) and reversed phase (RP) in the second dimension (<sup>2</sup>D) has been 66 67 shown to be characterized by a high degree of orthogonality for the analysis of complex 68 food samples [5], providing with complementary retention. Although in these two 69 separation modes the same types of mobile phases are employed, their coupling can be termed as fairly incompatible, considering that the relative solvent strength is the oppositein each mode, thus, producing serious solvent mismatch.

72 In a LC  $\times$  LC system, both dimensions are physically connected through the modulator. 73 The most-widely employed modulator so far is based on the use of one or more switching 74 valves equipped with two identical volume sampling loops [6]. This configuration allows 75 the effective collection and injection of discrete <sup>1</sup>D effluent fractions into the <sup>2</sup>D 76 continuously, by alternating the position and function of the two sampling loops. To 77 translate this into practice, different analytical conditions should be established, mainly: i) a <sup>1</sup>D slow separation based on the use of very low flow rates, in order to minimize, as 78 much as possible, the effluent fraction volume collected, and; ii) a fast <sup>2</sup>D using very high 79 80 flow rates, in order to achieve fast separations in the shortest possible analysis time to 81 allow a high <sup>1</sup>D sampling rate. As a consequence, set-ups involving the use of microbore columns in the <sup>1</sup>D combined with short wider columns (e.g., 4.6 mm i.d.) in the <sup>2</sup>D have 82 83 provided good results [5]. This type of coupling implies the additional advantage of injecting relatively small volumes of <sup>1</sup>D effluent on the <sup>2</sup>D, thus, reducing possible band 84 85 broadening. However, the main limitation directly related to the application of this 86 approach is the characteristic low sensitivity obtained in LC × LC compared to regular 87 one-dimensional methods, although potential deleterious issues due to solvent mismatch 88 are significantly reduced [7].

To partially alleviate these problems, different modulators have been designed; among them, thermal modulators are included. Within this group, several improvements have been presented, such as a vacuum-assisted evaporation interface aimed to remove the solvent from the <sup>1</sup>D effluent prior transfer to the <sup>2</sup>D [8], or the development of an oncolumn thermal modulation device [9]. This latter device was shown to be able to apply heating and cooling cycles to capture and elute analytes to the <sup>2</sup>D producing narrower

95 bands. However, due to their sophisticated and complicated design, these thermal 96 modulators have not been to date extended to other applications. In parallel, new 97 approaches have been explored taking advantage of the higher robustness and simplicity 98 of valve-based modulation, such as the use of two parallel <sup>2</sup>D columns [ref 10]. Another 99 interesting possibility to enhance the performance is to substitute the regular sampling 100 loops by trapping columns [10-12]. By using this approach, analytes are adsorbed by the 101 stationary phase of the trap, typically with similar selectivity to that found in the <sup>2</sup>D, 102 during the collection position, and are then eluted by the <sup>2</sup>D mobile phase in the injection position. Although, theoretically, the injection in <sup>2</sup>D mobile phase could also help to 103 produce narrow bands and even focusing at the top of the <sup>2</sup>D column, there still may exist 104 105 solvent incompatibility issues that may imply that not all the analytes contained in the  ${}^{1}D$ 106 effluent are efficiently retained in the trap. To overcome this issue, a modulation 107 procedure termed "active modulation" has recently been reported [13]; this approach is 108 based on the introduction of a make-up flow of a weaker solvent after <sup>1</sup>D separation and 109 before entrance to the trapping column. This way, a reduction in the solvent strength is 110 fostered, increasing the retention of the trap towards the compounds separated in the <sup>1</sup>D. 111 Subsequently, when the valve is actuated, those retained analytes can be eluted from the trap in narrow bands thanks to the <sup>2</sup>D mobile phase. From this basic procedure, other 112 113 modifications can be performed in order not only to improve the transfer of <sup>1</sup>D effluent 114 to the <sup>2</sup>D, but also to increase sensitivity and decrease analysis time. Although this active 115 modulation approach retains a high potential for the analysis of complex samples, its 116 applicability to food samples is still not demonstrated.

For this reason, the goal of the present work is to explore new possibilities to improve the separation of complex food samples, looking for quantitative improvements on resolving power, avoiding <sup>2</sup>D band broadening, as well as on sensitivity, using licorice as model 120 matrix. To this aim, different modifications at the modulator level are tested and 121 compared, studying their applicability on a HILIC  $\times$  RP coupling. The influence of the 122 separation and modulation parameters applied on the separation and detection of the 123 secondary metabolite profile of licorice, previously developed in our lab [14], including 124 glycosylated flavanones and chalcones and other polyphenols as well as triterpene 125 saponins, is evaluated.

126

127 2. MATERIALS AND METHODS.

# 128 **2.1. Samples and chemicals.**

Licorice samples (*Glycyrrhiza glabra*) from the region of Calabria, Italy, were collected in July 2015 and supplied from a local producer. For the extraction of secondary metabolites from this sample, a simple procedure based on solid-liquid extraction assisted by ultrasounds extraction was followed, as described before [15]. The extraction solvent was a binary mixture ethanol/water (1:1, v/v) using a sample-to-solvent ratio 1:5 (w/v) during 60 min. The resulting extract was filtered and evaporated to dryness. Prior injection, the extract was redissolved in water/acetonitrile (3:7, v/v).

HPLC grade ethanol and acetonitrile were purchased from VWR Chemicals (Barcelona,
Spain) whereas ultrapure water was produced from a Milli-Q instrument (Millipore,
Billerica, MA). Acetic and formic acids were supplied from Sigma-Aldrich (Madrid,

139 Spain), while ammonium acetate was from Panreac (Barcelona, Spain).

140

#### 141 **2.2. Instrumentation.**

The LC × LC-DAD instrumentation consisted on a first dimension (<sup>1</sup>D) composed by an
Agilent 1200 series liquid chromatograph (Agilent Technologies, Santa Clara, CA)
equipped with an autosampler. A Protecol flow-splitter (SGE Analytical Science, Milton

Keynes, UK) was installed between the <sup>1</sup>D pumps and the autosampler in order to 145 146 minimize the gradient delay volume of the pump and to obtain more reproducible low 147 flow rates. The second dimension (<sup>2</sup>D) was composed by an additional LC pump (Agilent 148 1290 Infinity). Both dimensions were connected by an electronically-controlled two-149 position ten-port switching valve (Rheodyne, Rohnert Park, CA, USA) acting as 150 modulator equipped with two identical sampling loops or trap columns, as indicated. A 151 diode array detector was coupled after the second dimension in order to register every <sup>2</sup>D 152 analysis. The system was simultaneously controlled by two different PC running 153 appropriate ChemStation software; one controlled the <sup>1</sup>D, the autosampler and DAD, whereas the other controlled the <sup>2</sup>D and actuated the switching valve. For the separations 154 155 involving the use of a make-up flow, a third LC pump (Agilent 1200 Series) was 156 connected through a t-piece between the outlet of <sup>1</sup>D and the switching valve. The used additional make-up flow was delivered at five-, seven- and nine-times the <sup>1</sup>D flow rate, 157 158 as indicated.

The LC linear chromatograms were elaborated and visualized as 2D- and 3D-plots using
LC Image software (version 1.0, Zoex Corp., Houston, TX).

161

162 **2.3. HILIC × RP separation conditions.** 

163 Different conditions and column combinations were employed during this research, as 164 described in Section 3. The common analytical conditions for each column used in the <sup>1</sup>D 165 were the following:

i) SeQuant ZIC-HILIC (150 × 1 mm, 3.5 μm, Merck, Darmstadt, Germany) column,
eluted using (A) acetonitrile and (B) 10 mM ammonium acetate at pH 5.0 as mobile
phases, according to the following gradient: 0 min, 3% B; 5 min, 3% B; 10 min, 5% B;
15 min, 10% B; 30 min, 20% B; 40 min, 20% B; 50 min, 30% B; 60 min, 30% B; 65 min,

170 40% B; 80 min, 40% B. The injection volume was 5  $\mu$ L and the flow rate was set at 15 171  $\mu$ L min<sup>-1</sup>.

ii) ZIC-HILIC ( $250 \times 2.1$  mm,  $3.5 \mu$ m, Merck, Darmstadt, Germany) column, eluted using (A) acetonitrile and (B) 10 mM ammonium acetate at pH 5.0 as mobile phases, according to the following gradient: 0 min, 3% B; 10 min, 3% B; 30 min, 10% B; 50 min, 15% B; 60 min, 20% B; 90 min, 40% B. The injection volume was 15 µL and the flow rate was set at 100 µL min<sup>-1</sup>.

177

On the other hand, the common analytical conditions for each column used in the <sup>2</sup>D were
the following:

i) Ascentis Express  $C_{18}$  (50 × 4.6 mm, 2.7 µm, Supelco, Bellefonte, CA) partially porous column using (A) water (0.1% formic acid) and (B) acetonitrile as mobile phases, eluted

182 at 3 mL min<sup>-1</sup> using two segment gradients: from 0 min to 23.4 min the  $^{2}$ D gradient elution

183 was 0 min, 0% B, 0.1 min, 5% B; 0.5 min, 35% B; 0.9 min, 70% B; 1 min, 90% B; 1.01

184 min, 0% B; 1.3 min, 0% B; from 23.4 to 80 min the employed gradient was programmed

185 as 0 min, 0% B; 0.1 min, 5% B; 0.3 min, 35% B; 0.5 min, 40% B; 0.9 min, 50% B; 1 min,

186 90% B; 1.01 min, 0% B; 1.3 min, 0% B.

187 ii) Ascentis Express  $C_{18}$  (30 × 4.6 mm, 2.7 µm, Supelco, Bellefonte, CA) partially porous 188 column using (A) water (0.1% formic acid) and (B) acetonitrile as mobile phases, eluted 189 at 2 mL min<sup>-1</sup>. Different gradients were applied depending on the modulation time 190 applied. The different step gradients are detailed in Table S1.

191

When indicated, sets of trapping columns formed by two identical cartridges were employed including  $C_{18}$  and phenyl-hexyl (10 × 3 mm, 2.6 µm, Accucore, Thermo Scientific, Waltham,MA) stationary phases. 195 UV-Vis spectra were collected in the range of 190-550 nm using a sampling rate of 20

Hz, while 254, 280 and 330 nm signals were also independently recorded.

197

# 198 **2.4. Calculations.**

199 2.4.1 Peak capacity.

200 Individual peak capacity for each dimension  $(n_c)$  was calculated according to eq. 1:

$$201 \qquad n_c = 1 + \frac{t_G}{\overline{w}} \tag{1}$$

202 where t<sub>G</sub> is the gradient time and  $\overline{w}$  is the average peak width. For <sup>1</sup>D peak capacity 203 calculations, the average peak width was obtained from *ca*. 10 representative peaks selected along the analysis. Likewise, for <sup>2</sup>D peak capacity, as much as possible peaks 204 were considered (*ca.* 20 peaks, depending on the analysis). Additionally,  ${}^{1}n_{c}$  was also 205 206 calculated considering the peak broadening factor  $\langle \beta \rangle$ , giving rise to a corrected <sup>1</sup>D peak 207 capacity (eq. 2), that considers the influence of the deleterious effect of undersampling. 208 To estimate  $\langle \beta \rangle$ , the sampling time (t<sub>s</sub>) as well as the average width of <sup>1</sup>D peaks as standard deviation in time units  $({}^{1}\sigma)$  before modulation were considered: 209

$$210 \qquad {}^{1}n_{c,corrected} = \frac{{}^{1}n_{c}}{\sqrt{1+0.21\left(\frac{t_{s}}{1_{\sigma}}\right)^{2}}} \tag{2}$$

For each two-dimensional set-up, different peak capacity values were estimated. First of
all, theoretical peak capacity was obtained following the so-called product rule, using eq.
3, considering the individual peak capacities obtained in each dimension:

$$214 \quad {}^{2D}n_{c,theoretical} = {}^{1}n_c \times {}^{2}n_c \tag{3}$$

As eq. 3 does not take into consideration the deleterious effects due to the modulation process as well as possible undersampling, a more realistic peak capacity value was obtained from the equation proposed by Li et al. [16] denominated here as practical peak capacity (eq. 4):

219 
$${}^{2D}n_{c,practical} = \frac{{}^{1}n_{c} \times {}^{2}n_{c}}{\sqrt{1+3.35 \times \left(\frac{{}^{2}t_{c}}{1}n_{c}}{1}\right)^{2}}$$
 (4)

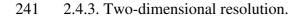
being  ${}^{2}t_{c}$ , the  ${}^{2}D$  separation cycle time, which is equal to the modulation time. This latter equation also includes the  $\langle\beta\rangle$  parameter accounting for undersampling. Moreover, to more precisely compare among set-ups and in order to evaluate possible peak clusters along the 2D analysis and, thus, to estimate 2D space coverage, the orthogonality degree  $(A_{O})$  was considered to offer the denominated 2D corrected (also known as effective) peak capacity, as follows:

$$226 \qquad {}^{2D}n_{c,corrected} = {}^{2D}n_{c,practical} \times A_0 \tag{5}$$

227

228 2.4.2 Orthogonality.

229 Among the different approaches that have been described and published to quantify the 230 orthogonality degree of a two-dimensional set-up [17], the method proposed by 231 Camenzuli and Schoenmakers [18] was employed in the present work to calculate system 232 orthogonality  $(A_0)$ . This procedure takes into account the spread of each peak along the 233 four imaginary lines that cross the 2D space forming an asterisk, that is  $Z_1$ ,  $Z_2$  (vertical 234 and horizontal lines) and Z<sub>-</sub>, Z<sub>+</sub> (diagonal lines of the asterisk). Z parameters describe the 235 use of the separation space with respect to the corresponding Z line, allowing to semi-236 quantitatively diagnose areas of the separation space where sample components are 237 clustered, thus, reducing in practice orthogonality. For the determination of each Z 238 parameter, the  $S_{Zx}$  value was calculated, as the measure of spreading around the  $Z_x$  line, 239 using the retention times of all the separated peaks in each 2D analysis.



The resolution metric for two-dimensional separations proposed by Peters et al. [19] was employed to calculate a representative resolution value and the separation quality of each set-up. This measure is based on the valley-to-peak ratio between two neighbor peaks. To establish the valley-to-peak ratio between two peaks (peak 1 and peak 2), three maximum intensities are considered: the maximum of the peak 1 (max1), the saddle point between both peaks (S) and the maximum of peak 2 (max2), as well as the distances between max1 and S,  $d_{1,S}$ , and the distance between S and max2,  $d_{S,2}$ .

249 
$$d_{1,S} = \sqrt{\left(\Delta^{1} t_{R1,S}\right)^{2} + \left(\Delta^{2} t_{R1,S}\right)^{2}}$$
 (6)

250 
$$d_{1,S} = \sqrt{\left(\Delta^{1} t_{RS,2}\right)^{2} + \left(\Delta^{2} t_{RS,2}\right)^{2}}$$
 (7)

where  $\Delta^{1} t_{R1,S}$  and  $\Delta^{2} t_{R1,S}$  are the differences on time between max1 and S in the <sup>1</sup>D and <sup>2</sup>D and  $\Delta^{1} t_{RS,2}$  and  $\Delta^{2} t_{RS,2}$  the difference between S and max2 in both dimensions.

253 Then, the intensity g is defined in accordance with the graphic showed in Figure S1.

254 Intensity *g* is calculated by:

255 
$$g = \frac{d_{1,S}h_{max2} + d_{S,2}h_{max1}}{d_{1,S} + d_{2,S}}$$
(8)

where  $h_{max1}$  and  $h_{max2}$  are the maximum intensities of peak 1 and peak 2, respectively.

257 The valley-to-peak ratio (V) is calculated as:

258 
$$\mathbf{V} = \frac{f}{g} = \frac{(g-h_s)}{g} \tag{9}$$

259 Finally, resolution (*Rs*) is estimated by the following equation:

260 
$$Rs = \sqrt{-\frac{1}{2} \ln\left(\frac{1-V}{2}\right)}$$
 (10)

In this work, the resolution measurement of two target critical pairs of peaks was calculated in each instrumental configuration, and results obtained compared among them.

#### 265 **3. RESULTS AND DISCUSSION**

266 In our previous work, the first  $LC \times LC$  application devoted to the profiling of secondary 267 metabolites in licorice was developed [14]. Although the method was characterized by 268 excellent separation capabilities, being possible to detect around 80 compounds from 269 different metabolite families in just one sample, further optimization is desirable to 270 increase sensitivity and to further improve performance. This is mainly interesting due to 271 the fact that this sample is a very diverse and complex mixture of some closely related 272 components, such as glycosylated flavanones and chalcones among other polyphenols as 273 well as triterpene saponins. In the present work, we have applied several strategies, using 274 licorice as a model complex real food sample in order to quantitatively evaluate the 275 attainable performance by introducing new changes in the interface.

276

#### 277 **3.1. Non-focusing modulation.**

278 3.1.1. Influence of transfer volume/fraction solvent.

279 The most-extended approach to interface both dimensions in  $LC \times LC$  is the use of two 280 identical sampling loops installed on the switching valve(s) acting as modulator. In our 281 original method, two 30 µL sampling loops were employed with satisfactory results. 282 However, modifications at the interface and columns combination levels could further 283 improve two of the most important points in a comprehensive LC separation: <sup>1</sup>D 284 undersampling and <sup>2</sup>D band broadening. These two parameters have a clear deleterious 285 effect both on the resolving power as well as on the attainable peak capacity, and thus, 286 should be minimized. The coupling between HILIC and RP is characterized by a very 287 good degree of orthogonality, thus, being very attractive for the analysis of complex 288 samples. Nevertheless, it generates a solvent mismatch during the transfer of <sup>1</sup>D effluent, considering that the weaker solvent in the <sup>1</sup>D is the stronger one on the <sup>2</sup>D environment. 289

According to the intensity of this issue, the resulting <sup>2</sup>D separations may be completely 290 291 ruined, or just worsened to a certain degree depending on the extent of the associated 292 band broadening effect. For this reason, one of the possible strategies to avoid or reduce 293 the mentioned solvent strength mismatch is to dilute the <sup>1</sup>D effluent before its transfer to 294 the <sup>2</sup>D. When using a non-focusing modulation procedure based on sampling loops, this 295 effect may be obtained through the use of loops with an internal volume higher than the 296 strictly required to collect the <sup>1</sup>D effluent during the length of a modulation. That way, 297 <sup>1</sup>D effluent supposes only part of the available loop volume whereas the rest is filled with 298 <sup>2</sup>D starting mobile phase. However, it has to be also considered that, since short columns 299 are employed in the <sup>2</sup>D to obtain fast separations, the increase on the sampling loop 300 volume, which is also the injection volume for each individual <sup>2</sup>D separation, may 301 negatively influence the separation [20].

302 Accordingly, the first step was to study the effects of sampling volume and fraction 303 solvent on the <sup>2</sup>D, comparing the separation attainable using sampling loops with different 304 internal volume, i.e., 20, 30 and 50 µL, operated in forward elution. To do that, 305 experimental conditions based on the use of the ZIC-HILIC microbore column in the <sup>1</sup>D 306 and the use of a 50  $\times$  4.6 mm, 2.7  $\mu$ m C<sub>18</sub> partially porous column in the <sup>2</sup>D, using 78 s 307 as modulation and <sup>2</sup>D analysis time, were applied (see Section 2.3). As can be observed 308 in Table 1 and Figure S2A-C, the results in terms of overall separation, resolution and 309 orthogonality were fairly similar. Interestingly, a slight but noticeable increase on 310 theoretical peak capacity was obtained when the sampling loops volume was bigger. This 311 trend would correspond to a decrease on average <sup>2</sup>D peak widths as a result of higher 312 dilution of the <sup>1</sup>D effluent and, thus, to the injection of each fraction on a weaker solvent, 313 which helps to improve peak shapes with respect to less diluted fractions. As can be also 314 observed in Table 1, 50 µL fractions injected in the <sup>2</sup>D meant an injection volume of 10%

315 of column void volume, considering that partially porous particles may occupy around 316 40% of the total available column inner volume [21,22]. Thus, the reduction on the 317 fraction solvent strength obtained when using 50 µL sampling loops (a 2.6-fold dilution) 318 was able to make up for the possible deleterious effect due to increased injection volume. 319 In fact, the use of 10% column void volume was significantly higher than the 3% 320 previously reported in order to not get peak distortion [20]. In spite of the increment 321 obtained in theoretical peak capacity, no practical gains on separation were observed 322 (Figure S2A-C).

323

324 3.1.2. Influence of sampling frequency.

325 Possible enhancements on resolving power could be obtained minimizing the effect of <sup>1</sup>D 326 undersampling. One of the concepts that characterize the performance of an on-line LC  $\times$ 327 LC method is the importance of maintaining the separation obtained in the <sup>1</sup>D during the 328 transfer of <sup>1</sup>D effluent to the <sup>2</sup>D. If the sampling process is too slow to collect fractions 329 where two well separated <sup>1</sup>D peaks are involved, undersampling arises; in that case, a 330 remix of these previously separated peaks occurs in the transfer process, producing a loss 331 of the <sup>1</sup>D separation and peak capacity. To reduce this negative effect, higher sampling frequencies should be applied, in order to obtain more  ${}^{1}D$  fractions analyzed in the  ${}^{2}D$ . 332 333 Murphy et al. [23] established the widely-accepted rule of sampling 3-4 times each <sup>1</sup>D 334 peak to solve the remix problem and to maintain the <sup>1</sup>D separation. However, in this case, 335 due to instrumental limitations on maximum bearable backpressure, it was not possible 336 to reduce the analysis time used with the 50 mm  $C_{18}$  partially porous column employed. 337 Changes in the <sup>2</sup>D gradient did not produce any noticeable improvement either. For this 338 reason, an even shorter column was tested. A  $30 \times 4.6$  mm C<sub>18</sub> partially porous column 339  $(2.7 \ \mu m)$  was coupled to the formerly optimized <sup>1</sup>D. By using this shorter column, a

proper separation was obtained allowing a decrease on total <sup>2</sup>D analysis time (gradient 340 341 time + re-equilibration time) to just 60 s. Under these analytical conditions, the use of the 342 three different transfer volumes was studied (Figure S2D-F). As can be observed from 343 the data summarized in Table 1, theoretical peak capacities obtained using the 30 mm 344 column were lower than those attainable using the 50 mm, as a result of the great 345 dependence of  ${}^{2}n_{c}$  on the available gradient time. However, as a result of the faster {}^{1}D 346 sampling rate applied when the shorter column was used, both orthogonality and 347 resolution of pair 1 were improved, independently of the transfer volume employed (see 348 Table 1). This improvement was more pronounced when using 50 µL sampling loops, as 349 deduced from the data shown on Table 1 and illustrated in Figure 1A-B and Figure S2. In 350 this latter set-up, the <sup>2</sup>D injection volume was equal to 17% of column void volume. 351 Although this relative injection volume is rather high, no appreciable distorted peaks were 352 detected compared to 20 and 30 µL transfer volumes; indeed, the dilution effect achieved 353 using 50 µL, again allowed better retention of compounds due to the greater dilution in 354 <sup>2</sup>D compatible mobile phase could produce a better interaction of the analytes with the 355 stationary phase (see Figure S2D-F and Figure S3).

356 Although these conditions clearly improved the results attainable using the longer 357 column, the use of higher separation temperature was also explored to investigate if proper <sup>2</sup>D separations could be obtained in even shorter analysis times, thus, further 358 359 increasing <sup>1</sup>D sampling rate. To do that, the <sup>2</sup>D column was thermostated at 40 °C and 360 several changes were applied to the gradient profile to adapt the separation to a total 39 361 and 50 s analysis times (Table S1). In order to establish a wider evaluation, the results 362 obtained using the different mentioned modulation times (39, 50 and 60 s) were also compared with the longer 78 s <sup>2</sup>D modulation time previously employed with the 50 mm 363 364 column. In this regard, considering that faster <sup>1</sup>D sampling rates imply that less <sup>1</sup>D

effluent volume is transferred to the  ${}^{2}D$ , the use of sampling loops volume of 50  $\mu$ L was 365 366 considered too high; for this reason, to perform these series of experiments, 20 µL 367 sampling loops were installed in the switching valve, allowing more discrete transfers 368 equivalent to 7% of total <sup>2</sup>D column void volume. Results are summarized in Table S2 and Figure 2. As can be observed, as the modulation time was reduced,  ${}^{2}n_{c}$  values also 369 370 decreased, as a result of the great influence that this value retains from the available <sup>2</sup>D 371  $t_{G}$ . In consequence, the practical 2D peak capacity also tended to decrease. However, the 372 observed decrease is not more pronounced thanks to the better peak shapes obtained as a 373 result of a more pronounced gradient slope and higher dilution effect when using 39 s as modulation time; at those conditions, just 9.5  $\mu$ L of <sup>1</sup>D effluent were transferred in each 374 375 modulation, whereas the rest of the sampling volume was filled with <sup>2</sup>D mobile phase, 376 thus, helping to reduce the solvent strength mismatch. Moreover, the effect of higher 377 sampling rate is also illustrated on the attainable resolution between the two pairs of 378 compounds studied. As illustrated in Figure 2, resolution between pair 1 improved when 379 reducing the modulation time. In addition, compounds in pair 2 remained coeluted using 380 modulation times of 78 and 60 s, but they could be separated using shorter modulation 381 times.

382

# **383 3.2. Focusing modulation using trapping columns.**

One of the possible implementations to reduce <sup>2</sup>D band broadening and to increase sensitivity limiting dilution is the use of trapping columns in the valve-based modulator. Reduction on band broadening is accomplished by introducing a focusing effect, considering that the analytes eluting from the <sup>1</sup>D would be entrapped in the trapping column during the collection position. Once the valve is actuated, <sup>2</sup>D mobile phase would desorb the analytes in discrete bands, injecting them into the <sup>2</sup>D column. Even if this

390 approach has a good potential, its use is very limited compared to regular loops-based 391 modulation. In the food analysis field, only C<sub>18</sub> trapping columns have been reported [10,24], in order to exactly match the selectivity of the  $^{2}$ D column. In the present work, 392 393 the use of trapping columns-based modulation to increase resolving power and sensitivity 394 is extended to other stationary phases. Namely, the use of  $C_{18}$  and phenyl-hexyl trapping 395 columns have been explored. The traps  $(10 \times 3.0 \text{ mm}, 2.6 \mu\text{m})$  were installed in the 396 modulator using the minimum possible extra volume for connections. The trapping 397 columns void volume was 42 µL. Moreover, two elution configurations were compared, namely, forward and backflush elution. The use of the shortest available <sup>2</sup>D column was 398 399 maintained, setting a modulation time of 60 s. Table 2 reports the most important method 400 parameters related to these analyses. As can be observed, very similar results could be 401 obtained using the two stationary phases available as well as both elution modes in terms 402 of peak capacity and orthogonality attainable. Interestingly, using both elution modes 403 resolution of critical pair 1 was maintained with respect to the best value attainable using 404 non-focusing modulation, whereas, pair 2, that coeluted using the same separation 405 conditions (60 s modulation time) with sampling loops, was also resolved. In any case, 406 forward elution produced better resolution results for both tested stationary phases. Moreover, as can be appreciated from Figure S4, in general, <sup>2</sup>D peak shapes were 407 408 improved also under forward elution compared to backflush elution. This effect would be 409 obtained as a result of the longer available interaction allowed under forward elution, 410 bearing in mind that the trapping column was not fully filled with <sup>1</sup>D effluent during the 411 collection position (see Figure 3A,B). In addition, although reduced to a minimum, a 2 412 µL tube was necessary to connect the trapping columns to the valve; consequently, there 413 was a small fraction of <sup>1</sup>D effluent that did not enter the trapping column when backflush 414 elution was employed (Figure 3B).

415

# 416 **3.3. Focusing using active modulation.**

417 The use of active modulation is a further evolution of the direct use of trapping columns. 418 This modulation procedure, recently proposed [13], is based on the use of an additional 419 make-up flow of a weak solvent for the <sup>2</sup>D in order to reduce the strength of the <sup>1</sup>D effluent 420 prior entering the trapping column. This way, the interaction between the analytes and 421 the functional groups in the trap is fostered, as illustrated in Figure 3C. Therefore, 422 considering the high potential and relative simplicity that this implementation may have, 423 it is worth to study its application to complex food samples. Considering the  ${}^{1}D$  and  ${}^{2}D$ 424 mobile phases compositions, it was decided to use ultrapure water (0.1% formic acid) as 425 make-up flow. It has been previously observed that a flow rate for the additional make-426 up flow 7-times higher than the <sup>1</sup>D flow rate was appropriate to achieve the desired effect 427 [13]. However, to further study the possible influence of make-up flow rate on the overall 428 separation performance, three different flow rates for each set of trapping columns ( $C_{18}$ 429 and phenyl-hexyl) were tested, i.e., 5-, 7- and 9-times the <sup>1</sup>D flow rate. Table 3 430 summarizes the data describing the performance attained using active modulation for the 431 profiling of secondary metabolites in licorice. As can be appreciated, as for trapping 432 columns, the performance attainable using both stationary phases was very similar. In 433 both cases, the use of higher make-up flow rates allowed a slight improvement on peak 434 capacity, whereas orthogonality values were essentially maintained. More relevant was 435 the improvement observed for the resolution between the two studied pairs; in this regard, 436 the use of make-up flow rates 9-times higher than the <sup>1</sup>D flow rate produced the best 437 results (Figure 4).

438

## 439 **3.4. Overall comparison.**

440 As already described in the previous sections, different approaches have been considered 441 to further improve the separation capabilities of the initial HILIC × RP method directed 442 towards the profiling of secondary metabolites in licorice. In general, the use of focusing 443 modulation, either using trapping columns or active modulation, allowed a clear 444 improvement on the separation of the complex metabolite profile of this sample (Figure 445 1). In fact, these two approaches allowed obtaining good degrees of resolution between 446 the studied pairs (Figures 4 and S4). In general, better separations were obtained using 447 trapping columns in forward elution mode and using active modulation with make-up 448 flow rates 9-times the <sup>1</sup>D flow rate. Although in both cases, the two stationary phases 449 studied produced comparable performance, the phenyl-hexyl particles were slightly better 450 than  $C_{18}$  particles. Under these conditions, similar orthogonality values as well as 451 resolution between the critical pairs were obtained (Tables 2 and 3). However, practical 452 peak capacities were significantly higher using active modulation (2131 vs 1811), and 453 thus, this procedure resulted more favorable. The use of non-focusing modulation by 454 sampling loops could only provide comparable performance in some aspects when 455 modulation time was significantly reduced, thus, increasing <sup>1</sup>D sampling rate. However, 456 due to very fast <sup>2</sup>D separations, the total 2D peak capacity attainable was severely 457 compromised with respect to active modulation.

With the aim to further obtain more data illustrating the performance of each procedure, the attainable sensitivity under each separation conditions was studied by analyzing peak S (Figure 5). Values of normalized sensitivity for each set-up are included in Tables 1-3. This value was obtained by considering the sensitivity for peak S in the original method with respect to the sensitivity obtained in each case. As can be observed from those results, the set-up involving the use of active modulation using phenyl-hexyl traps and make-up flow at 9-time <sup>1</sup>D flow rate produced the highest sensitivity enhancement. 465 Consequently, active modulation was shown again as the best possible alternative set-up 466 for the profiling of secondary metabolites in licorice by HILIC  $\times$  RP in order to further 467 enhance both resolving power and sensitivity.

468 In this regard, theoretically, further sensitivity gains could be obtained if a column with 469 higher sample loadability is used in <sup>1</sup>D. For this reason, a last attempt was made using the 470 optimum separation conditions but increasing the <sup>1</sup>D column internal diameter to 2.1 mm. 471 That column allowed an increase on the injection volume to 15  $\mu$ L, although higher <sup>1</sup>D 472 flow rates were also needed to maintain the <sup>1</sup>D separation. This would have a deleterious effect on the fraction volume transferred to <sup>2</sup>D, but considering that active modulation 473 474 was employed with trapping columns, the fraction volume should not have such a critical 475 influence on the coupling. As shown in Table S3, the normalized sensitivity obtained was 476 further increased with respect to the use of the microbore <sup>1</sup>D column (Figure 5F); 477 however, the separation obtained was severely hampered, and the resolution between the 478 critical pairs studied was completely lost (Table S3). Thus, this modification was not 479 considered favorable, bearing in mind that compromises should be always taken between 480 sensitivity, resolving power and overall peak capacity obtainable.

481

482

# 483 **4. CONCLUSIONS.**

In the present contribution, different strategies are proposed and compared to further increase HILIC × RP method performance for the analysis of complex food samples, using licorice as a model sample. When using non-focusing modulation based on sampling loops, the use of very short columns (30 mm) in the <sup>2</sup>D was shown to be beneficial to increase performance, taking advantage of higher sampling loops volume to increase solvent dilution, thus, minimizing the deleterious effects due to solvent strength 490 mismatch between HILIC and RP. However, the use of focusing modulation procedures 491 was demonstrated to be able to increase not only resolving power but also peak capacity, 492 reducing the effects of solvent mismatch at the same time that producing a focusing effect 493 at the beginning of the <sup>2</sup>D analyses. In addition, significant sensitivity gains could be also 494 obtained through the use of active modulation with a relatively high make-up flow rate. 495 A total of 94 peaks were successfully separated in the set-up involving the use of active 496 modulation with phenyl-hexyl trapping columns and a make-up flow rate 9-times higher 497 than the corresponding <sup>1</sup>D flow rate, compared to the initial method (79 peaks), increasing 498 sensitivity more than twice. In summary, the results obtained demonstrate the great 499 applicability and potential that active modulation may have for the profiling of complex 500 food samples by HILIC  $\times$  RP.

501

502

# 503 ACKNOWLEDGEMENTS.

504 The authors would like to thank Project AGL2014-53609-P (MINECO, Spain) for 505 financial support.

# 506 **REFERENCES.**

- 507 [1] P.Q. Tranchida, P. Donato, F. Cacciola, M. Beccaria, P. Dugo, L. Mondello.
- 508 Potential of comprehensive chromatography in food analysis, TrAC Trends Anal.
- 509 Chem. 52 (2013) 186-205.
- 510 [2] M. Sarrut, G. Cretier, S. Heinisch. Theoretical and practical interest in UHPLC
- 511 technology for 2D-LC. TrAC Trends Anal. Chem. 63 (2014) 104-112.
- 512 [3] X. Shi, S. Wang, Q. Yang, X. Lu, G. Xu, Comprehensive two-dimensional
- 513 chromatography for analyzing complex samples: Recent new advances, Anal. Methods
- 514 6 (2014) 7112-7123.
- 515 [4] F. Bedani, P.J. Schoenmakers, H.G. Jansen. Theories to support method
- 516 development in comprehensive two-dimensional liquid chromatography a review, J.
- 517 Sep. Sci. 35 (2012) 1697-1711.
- 518 [5] F. Cacciola, S. Farnetti, P. Dugo, P.J. Marriott, L. Mondello, Comprehensive two-
- dimensional liquid chromatography for polyphenol analysis in foodstuffs, J. Sep. Sci. 40(2017) 7-24.
- 521 [6] M.J. Egeness, M.C. Breadmore, E.F. Hilder, R.A. Shellie. The modulator in
- 522 comprehensive two-dimensional liquid chromatography. LC-GC Eur. 5 (2016) 268-276.
- 523 [7] F. Cacciola, P. Donato, D. Giuffrida, G. Torre, P. Dugo, L. Mondello. Ultra high
- 524 pressure in the second dimension of a comprehensive two-dimensional liquid
- 525 chromatographic system for carotenoid separation in red chili peppers, J. Chormatogr.
- 526 A 1255 (2012) 244–251.
- 527 [8] H. Tian, J. Xu, Y. Guan. Comprehensive two-dimensional liquid chromatography
- 528 (NPLC x RPLC) with vacuum-evaporation interface, J. Sep. Sci. 31 (2008) 1677–1685.

- 529 [9] M.E. Creese, M.J. Creese, J.P. Foley, H.J. Cortes, E.F. Hilder, R.A. Shellie, M.C.
- 530 Breadmore. Longitudinal On-Column Thermal Modulation for Comprehensive Two-
- 531 Dimensional Liquid Chromatography, Anal. Chem. 89 (2017) 1123–1130.
- 532 [10] F. Cacciola, P. Jandera, E. Blahovà, L. Mondello, L. Development of different
- 533 comprehensive two-dimensional systems for the separation of phenolic antioxidants, J.
- 534 Sep. Sci. 29 (2006) 2500–2513.
- 535 [11] R.J. Vonk, A.F.G. Gargano, E. Davydova, H.L. Dekker, S. Eeltink, L.J. de
- 536 Koning, P.J. Schoenmakers. Comprehensive Two-Dimensional Liquid Chromatography
- 537 with Stationary-Phase-Assisted Modulation Coupled to High-Resolution Mass
- 538 Spectrometry Applied to Proteome Analysis of Saccharomyces cerevisiae, Anal. Chem.
- 539 87 (2015) 5387–5394.
- 540 [12] Y. Zhao, S.S. W. Szeto, R.P.W. Kong, C.H. Law, G. Li, Q. Qan, Z. Zhang, Y.
- 541 Wang, I.K. Chu. Online Two-Dimensional Porous Graphitic Carbon/Reversed Phase
- 542 Liquid Chromatography Platform Applied to Shotgun Proteomics and Glycoproteomics,
- 543 Anal. Chem. 86 (2014) 12172-12719.
- 544 [13] A.F. Gargano, M. Duffin, P. Navarro, P.J. Schoenmakers. Reducing dilution and
- 545 analysis time in online comprehensive two-dimensional liquid chromatography by
- 546 active modulation, Anal. Chem. 88 (2016) 1785-1793.
- 547 [14] L. Montero, E. Ibañez, M. Russo, R. di Sanzo, L. Rastrelli, A.L. Piccinelli, R.
- 548 Celano, A. Cifuentes, M. Herrero. Metabolite profiling of licorice (*Glycyrrhiza glabra*)
- 549 from different locations using comprehensive two-dimensional liquid chromatography
- 550 coupled to diode array and tandem mass spectrometry detection, Anal. Chim. Acta 913
- 551 (2016) 145-159.
- 552 [15] P. Montoro, M. Maldini, M. Russo, S. Postorino, S. Piacente, C. Pizza. Metabolic
- 553 profiling of roots of liquorice (*Glycyrrhiza glabra*) from different geographical areas by

- 554 ESI/MS/MS and determination of major metabolites by LC-ESI/MS and LC-
- 555 ESI/MS/MS, J. Pharm. Biomed. Anal. 54 (2011) 535-544.
- 556 [16] X. Li, D.R. Stoll, P.W. Carr. Equation for peak capacity estimation in two-
- dimensional liquid chromatography, Anal. Chem. 81 (2009) 845–850.
- 558 [17] M.R. Schure, J.M. Davis, Orthogonal separations: Comparison of
- orthogonalitymetrics by statistical analysis, J. Chromatogr. A 1414 (2015) 60-76.
- 560 [18] M. Camenzuli, P.J. Schoenmakers, A new measure of orthogonality for multi-
- 561 dimensional chromatography, Anal. Chim. Acta 838 (2014) 93–101.
- 562 [19] S. Peters, G. Vivó-Truyols, P.J. Marriott, P.J. Schoenmakers. Development of a
- 563 resolution metric for comprehensive two-dimensional chromatography, J. Chromatogr.
- 564 A, 1146 (2007) 232–241.
- 565 [20] P. Jandera, T. Hajek, P. Cesla. Effects of the gradient profile, sample volume and
- solvent on the separation in very fast gradients, with special attention to the second-
- 567 dimension gradient in comprehensive two-dimensional liquid chromatography, J.
- 568 Chromatrogr. A 1218 (2011) 1995-2006.
- 569 [21] F. Gritti, G. Guiochon. Theoretical investigation of diffusion along columns packed
- 570 with fully and superficially porous particles, J. Chromatogr. A, 1218 (2011) 3476-3488.
- 571 [22] R. Hayes, A. Ahmed, T. Edge, H. Zhang. Core-shell particles: Preparation,
- 572 fundamentals and applications in high performance liquid chromatography, J.
- 573 Chromatogr. A 1357 (2014) 36-52.
- 574 [23] R.E. Murphy, M.R. Schure, J.P. Foley. Effect of Sampling Rate on Resolution in
- 575 Comprehensive Two-Dimensional Liquid Chromatography, Anal. Chem.70 (1998)
- 576 1585–1594.

- 577 [24] F. Cacciola, P. Jandera, Z. Hajdù, P. Česla, L. Mondello, L. Comprehensive two-
- 578 dimensional liquid chromatography with parallel gradients for separation of phenolic
- 579 and flavone antioxidants, J. Chromatogr. A 1149 (2007) 73–87.

580

### 582 FIGURE LEGENDS

**Figure 1.** Resolution obtained for peaks included in critical pair 1 (white oval) and in critical pair 2 (black oval) in the different set-ups studied. A, using 50  $\mu$ L sampling loops in combination with a 50 mm long column in the <sup>2</sup>D; B, using 50  $\mu$ L sampling loops in combination with a 30 mm long column in the <sup>2</sup>D; C, using Phenyl-hexyl trapping columns with forward elution, and; D, using active modulation with phenyl-hexyl traps and make-up flow rate equal to 9-times <sup>1</sup>D flow rate.

589

**Figure 2.** Dependence of practical peak capacity  $({}^{2D}n_{c,\text{practical}})$  (•), 2D resolution reached

for pair 1 (•), and 2D resolution for pair 2 (×) on modulation time. For detailed separation
conditions, see section 2.3.

593

**Figure 3.** Hypothetical scheme of the retention/elution of secondary metabolites from licorice into the trapping columns under forward elution mode (A), backflush elution mode (B), and active modulation (C) set-ups studied, following the procedure: 1) Trapping column filled with <sup>2</sup>D initial mobile phase (injection position, just after valve actuation); 2) Trapping column filled with <sup>1</sup>D effluent fraction (collection position) diluted in strong (A and B) or weak (C) solvent; 3) start of <sup>2</sup>D gradient. Arrows indicate flow direction.

601

Figure 4. Resolution obtained by using active modulation with phenyl-hexyl trapping
columns of the two pairs of the studied peaks, using make-up flow rates equal to 5- (A),
7- (B) and 9-times (C) <sup>1</sup>D flow rate, and practical scheme of the calculation of the valleyto-peak ratio used for the estimation of resolution between critical pairs 1 and 2 (D).

- 607 **Figure 5.** Panel A: 2D-plot (254 nm) of the separation obtained in the original method.
- 608 Sensitivity comparison (peak S) of the original method with the set-up of each modulation
- 609 configuration using: B,  $50 \,\mu L$  sampling loops in combination with 50 mm length column
- 610 in the <sup>2</sup>D; C, 50  $\mu$ L sampling loops in combination with 30 mm length column in the <sup>2</sup>D;
- 611 D, C<sub>18</sub> trapping columns with forward elution; E, active modulation with phenyl-hexyl
- 612 traps and make-up flow rate equal to 9-times <sup>1</sup>D flow rate, and; F, sensitivity gain with
- 613 the 250 × 2,1 mm, 3,5  $\mu$ m <sup>1</sup>D column. (Retention times of analyses with different <sup>2</sup>D
- 614 gradient are aligned to help the comparison).

		$^{2}\text{D}$ - C <sub>18</sub> 50 × 4.6 mm, 2.7 µm			$^{2}$ D - C <sub>18</sub> 30 × 4.6 mm, 2.7 µm		
	Sampling loop volume	20 µL	30 µL	50 µL	20 µL	30 µL	50 µL
<sup>1</sup> D	L (mm)	150	150	150	150	150	150
	I.D. (mm)	1.0	1.0	1.0	1.0	1.0	1.0
	Particle size (µm)	3.5	3.5	3.5	3.5	3.5	3.5
	Flow rate ( $\mu L \min^{-1}$ )	15	15	15	15	15	15
	$\overline{w}$ (min)	2.69	2.69	2.69	2.47	2.47	2.47
	$^{1}n_{\rm c}$	30	30	30	33	33	33
	<β>	1.33	1.33	1.33	1.25	1.25	1.25
	$^{1}n_{\rm c}$ corr.	23	23	23	27	27	27
$^{2}D$	$\overline{w}$ (s)	1.06	0.90	0.78	1.02	1.00	1.00
	$^{2}n_{c}$	75	88	101	60	61	61
LC × LC	Analysis time (min)	80	80	80	80	80	80
	ts	1.93σ	1.93σ	1.93σ	1.62σ	1.62σ	1.62σ
	Modulation time (min)	1.3	1.3	1.3	1.0	1.0	1.0
	M – number of modulations	62	62	62	80	80	80
	<sup>2</sup> V <i>inj</i> (V dilution)	20 μL (0.5 μL)	30 µL (10.5 µL)	50 μL (30.5 μL)	20 μL (5.0 μL)	30 µL (15.0 µL)	50 μL (35.0 μL
	% <sup>2</sup> D column void volume	4%	6%	10%	7%	10%	17%
	Gradient delay volume (mL)	0.72	0.74	0.76	0.48	0.48	0.51
	<sup>2</sup> D column operation preassure (bar)	299	295	298	187	185	190
	$Z_1$	0,84	0,91	0,92	0,89	0,82	0,85
	$Z_2$	0,97	0,96	0,99	0,97	0,98	0,97
	Z.	0,69	0,77	0,81	0,91	0,89	0,86
	$Z_{+}$	0,83	0,87	0,84	0,99	0,95	0,99
	$A_O$	68%	76%	79%	82%	82%	84%
	Resolution pair 1	0.65	0.67	0.70	0.75	0.83	0.89
	Resolution pair 2	-	-	-	-	-	-
	Normalized sensitivity	0.85	1.00	1.37	1.08	1.32	1.61
	$^{2D}n_{c}$ theoretical	2250	2640	3030	1980	2013	2013
	$^{2D}n_{c}$ practical	1730	1964	2253	1706	1736	1780
	${}^{2D}n_{\rm c}$ corr.	1401	1493	1780	1399	1424	1495

615 Table 1. Comprehensive two-dimensional method parameters applied to the profiling of secondary metabolites from licorice using non-focusing
 616 modulation

- 618 619  $\langle\beta\rangle$ , average <sup>1</sup>D broadening factor; <sup>1</sup> $n_c$  corr.: calculated according to eq. 2; t<sub>s</sub>, sampling time;  $A_O$ , orthogonality; <sup>2D</sup> $n_c$  theoretical: <sup>1</sup> $n_c \times ^2 n_c$ ; <sup>2D</sup> $n_c$  practical: calculated according to eq. 4; <sup>2D</sup> $n_c$  corr.: <sup>2D</sup> $n_c \times A_O$

620 **Table 2.** Comprehensive two-dimensional method parameters applied to the profiling of

		Forwa	ard elution	Backflush elution		
	Trapping column	C18	Phenyl-hexyl	C18	Phenyl-hexyl	
<sup>1</sup> D	L (mm)	150	150	150	150	
	I.D. (mm)	1.0	1.0	1.0	1.0	
	Particle size (µm)	3.5	3.5	3.5	3.5	
	Flow rate (µLmin <sup>-1</sup> )	15	15	15	15	
	$\overline{w}$ (min)	2.11	2.11	2.11	2.11	
	$^{1}n_{c}$	39	39	39	39	
	<β>	1.32	1.32	1.32	1.32	
	${}^{1}n_{c}$ corr.	30	30	30	30	
$^{2}$ D	$\overline{W}(s)$	0.97	0.96	0.98	0.98	
	$^{2}n_{c}$	63	64	62	62	
$LC \times LC$	Analysis time (min)	80	80	80	80	
	ts	1.88σ	1.88σ	1.88σ	1.88 σ	
	Modulation time (min)	1.0	1.0	1.0	1.0	
	M – number of	80	80	80	80	
	modulations					
	Gradient delay volume	0.51	0.51	0.44	0.44	
	(mL)					
	<sup>2</sup> D column operation	260	258	253	254	
	preassure (bar)					
	$Z_1$	0,94	0,86	0,83	0,87	
	$Z_2$	0,92	0,94	0,97	0,93	
	Z.	0,94	0,89	0,92	0,97	
	$Z_{+}$	0,93	0,98	0,92	0,83	
	$A_0$	87%	84%	83%	81%	
	Resolution pair 1	0.80	0.80	0.79	0.81	
	Resolution pair 2	0.81	0.85	0.72	0.78	
	Normalized sensitivity	1.15	0.99	0.59	0.75	
	$^{2D}n_{\rm c}$ theoretical	2457	2496	2418	2418	
	$^{2D}n_{c}$ practical	1792	1811	1777	1777	
	$^{2D}n_{\rm c}$ corr.	1559	1521	1475	1439	

621 secondary metabolites from licorice using trapping columns-based focusing modulation.

622 <β>, average <sup>1</sup>D broadening factor; <sup>1</sup> $n_c$  corr.: calculated according to eq. 2; t<sub>s</sub>, sampling time;  $A_O$ , 623 orthogonality; <sup>2D</sup> $n_c$  theoretical: <sup>1</sup> $n_c$  ×<sup>2</sup> $n_c$ ; <sup>2D</sup> $n_c$  practical: calculated according to eq. 4; <sup>2D</sup> $n_c$  corr.: <sup>2D</sup> $n_c$  ×  $A_O$ 624

			C18 trapping column	S	Phe	Phenyl-hexyl trapping columns	
	Make-up flow rate	$5 \times {}^{1}F$	$7 \times {}^{1}F$	$9 \times {}^{1}F$	$5 \times {}^{1}F$	$7 \times {}^{1}F$	$9 \times {}^{1}F$
$^{1}D$	L (mm)	150	150	150	150	150	150
	I.D. (mm)	1.0	1.0	1.0	1.0	1.0	1.0
	Particle size (µm)	3.5	3.5	3.5	3.5	3.5	3.5
	<sup>1</sup> F (Flow rate, µL min <sup>-1</sup> )	15	15	15	15	15	15
	$\overline{w}$ (min)	2.11	2.11	2.11	2.11	2.11	2.11
	$^{1}n_{c}$	39	39	39	39	39	39
	<β>	1.33	1.33	1.33	1.32	1.32	1.32
	$^{1}n_{\rm c}$ corr.	1.32	1.32	1.32	1.32	1.32	1.32
$^{2}$ D	$\overline{w}(s)$	0.93	0.84	0.81	0.96	0.84	0.81
	$^{2}n_{c}$	66	73	75	63	73	75
$LC \times LC$	Analysis time (min)	80	80	80	80	80	80
	t <sub>s</sub>	1.88σ	1.88σ	1.88σ	1.88σ	1.88σ	1.88σ
	Modulation time (min)	1.0	1.0	1.0	1.0	1.0	1.0
	M – number of modulations	80	80	80	80	80	80
	Gradient delay volume (mL)	0.49	0.49	0.49	0.49	0.49	0.49
	Column operation preassure (bar)	266	267	266	259	261	262
	$Z_1$	0,87	0,89	0,90	0,87	0,87	0,88
	$Z_2$	0,98	0,96	0,96	0,96	0,94	0,94
	Z-	0,91	0,92	0,91	0,87	0,89	0,89
	Z+	0,93	0,93	0,94	0,96	0,97	0,95
	$A_O$	85%	86%	86%	84%	84%	84%
	Resolution pair 1	0.69	0.82	0.85	0.71	0.91	0.93
	Resolution pair 2	0.81	0.86	0.88	0.82	0.86	0.88
	Normalized sensitivity	1.46	1.59	1.98	0.91	1.67	2.01
	$^{2D}n_{\rm c}$ theoretical	2574	2847	2925	2457	2847	2925
	$^{2D}n_{\rm c}$ practical	1888	2075	2128	1806	2070	2131

Table 3. Instrumental parameters employed and method performance descriptors from the use of active modulation for the profiling of secondary

# 626 metabolites from licorice.

$^{2D}n_{\rm c}$ corr.	1605	1785	1830	1517	1739	1790

 $\beta$ , average <sup>1</sup>D broadening factor; <sup>1</sup> $n_c$  corr.: calculated according to eq. 2; t<sub>s</sub>, sampling time;  $A_O$ , orthogonality; <sup>2D</sup> $n_c$  theoretical: <sup>1</sup> $n_c \times {}^2n_c$ ; <sup>2D</sup> $n_c$  practical: calculated according to eq. 4; <sup>2D</sup> $n_c$  corr.: <sup>2D</sup> $n_c \times A_O$ 628